

A Closer Look at Temporal Sentence Grounding in Videos: Datasets and Metrics

Yitian Yuan¹ Xiaohan Lan² Long Chen³ Wei Liu⁴ Xin Wang⁵ Wenwu Zhu⁵

¹Tsinghua-Berkeley Shenzhen Institute, Tsinghua University

²Tsinghua Shenzhen International Graduate School, Tsinghua University

³Tencent AI Lab ⁴Tencent Data Platform

⁵ Department of Computer Science and Technology, Tsinghua University

Abstract

Despite Temporal Sentence Grounding in Videos (TSGV) has realized impressive progress over the last few years, current TSGV models tend to capture the moment annotation biases and fail to take full advantage of multi-modal inputs. Miraculously, some extremely simple TSGV baselines even without training can also achieve state-of-the-art performance. In this paper, we first take a closer look at the existing evaluation protocol, and argue that both the prevailing datasets and metrics are the devils to cause the unreliable benchmarking. To this end, we propose to re-organize two widely-used TSGV datasets (Charades-STA and ActivityNet Captions), and deliberately Change the moment annotation Distribution of the test split to make it different from the training split, dubbed as Charades-CD and ActivityNet-CD, respectively. Meanwhile, we further introduce a new evaluation metric “dR@n,IoU@m” to calibrate the basic IoU scores by penalizing more on the over-long moment predictions and reduce the inflating performance caused by the moment annotation biases. Under this new evaluation protocol, we conduct extensive experiments and ablation studies on eight state-of-the-art TSGV models. All the results demonstrate that the re-organized datasets and new metric can better monitor the progress in TSGV, which is still far from satisfactory. The repository of this work is at https://github.com/ytzsy/grounding_changing_distribution.

1. Introduction

Detecting activities of interest from untrimmed videos is a prominent and fundamental problem in video scene understanding. Early video action localization works [21, 27] mainly focus on detecting activities belonging to the predefined categories [21, 27], which extremely restrict their flexibility and extensibility. To address this issue, a challenging task that extends the limited categories to natural language queries was proposed [1, 6, 11], called **Temporal Sentence**

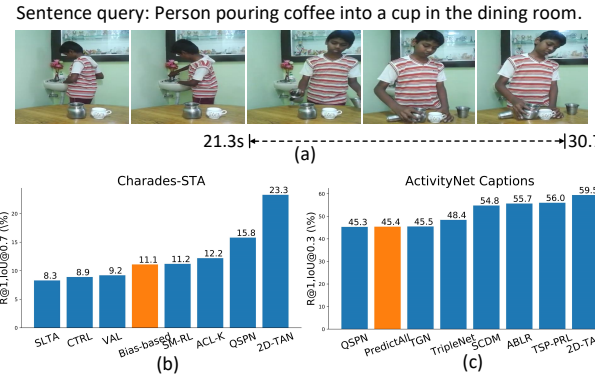


Figure 1. (a): TSGV aims to localize a moment with start and end timestamps in the video given a natural language query. (b): The performance comparisons of SOTA models on dataset Charades-STA with metric R@1,IoU@0.7. (c): The performance comparisons on dataset ActivityNet Captions with metric R@1,IoU@0.3.

Grounding in Videos (TSGV). As shown in Figure 1 (a), given a natural language query and an untrimmed video, TSGV needs to identify the start and end timestamps of one segment (or moment) in the video, which semantically corresponds to the language query. Due to its profound significance, the TSGV task has received unprecedented attention over the last few years — a surge of datasets [1, 6, 13, 20] and state-of-the-art (SOTA) methods [3, 4, 5, 7, 8, 9, 10, 12, 14, 15, 16, 28, 29, 30, 31, 32, 33, 34, 35, 36] have been developed.

Although each newly proposed method has been shown to make progress over previous ones, a recent study [18] shows that even today’s TSGV models still make very little use of visual inputs, *i.e.*, they are heavily driven by the biases in the ground truth moment annotations and lack sufficient multi-modal understanding. Specifically, taking the prevailing benchmark Charades-STA [6] as an example, suppose that there is a naive Bias-based model which only makes predictions by sampling a moment from the frequency statistics of the ground truth moments in the training

set. As shown in Figure 1 (b), the Bias-based model unexpectedly achieves competing and even better performance than several SOTA deep models. Thus, we argue that these datasets with biased annotations cannot accurately monitor the progress in TSGV.

To fairly benchmark each proposed method, another critical factor comes from the evaluation metrics. Currently, the most prevalent metric for TSGV is: $R@n, IoU@m$, i.e., the percentage of testing samples which have at least one of the top- n results with IoU larger than m . Due to the difficulty of the TSGV task, almost all published works tend to use a small threshold m (e.g., 0.3) to conduct the evaluation, especially for challenging datasets, e.g., ActivityNet Captions [13]. However, we argue that the metric $R@n, IoU@m$ with small m is unreliable for the datasets with biased annotations. For example, the ground truth moment annotations in the ActivityNet Captions usually have long durations (e.g., 40% queries refer to a moment occupy over 30% temporal ranges of the whole video). Therefore, a small IoU threshold can be easily reached by a long duration prediction. As an extreme case, a baseline directly takes the whole video as the prediction can still achieve SOTA performance under the metric with a small IoU threshold (Figure 1 (c)).

To help disentangle the effects of ground truth moment annotation biases, we present new splits of Charades-STA and ActivityNet Captions, called **Charades-CD** (Charades-STA under Changing Distributions) and **ActivityNet-CD**, respectively. These new splits are created by re-organizing all splits (i.e., the training, validation and test set) of original datasets, and the ground truth moment distributions are designed *different* in the training and test splits, i.e., out-of-distribution (OOD) testing. To better demonstrate the TSGV models’ generalization ability and compare the performance between the OOD samples and the independent and identically distributed (IID) samples, we also maintain a test split with IID samples, denoted as test-iid (vs. test-ood). Meanwhile, we propose a more reliable evaluation metric — $dR@n, IoU@m$ — for small thresholds m . This metric calibrates the basic IoU scores by penalizing more on the over-long moment predictions, which is expected to reduce the influence of moment annotations biases.

To demonstrate the difficulty of our new splits, we report the performance of several existing TSGV models on them. Our key finding is that the performance of most tested models drops significantly when evaluated on the OOD samples (i.e., the test-ood set) compared to the IID samples (i.e., the test-iid set). This finding provides a further confirmation that existing methods only fit the moment annotation biases, and fail to bridge the truly semantic correlation between the video contents and natural language queries. Meanwhile, the proposed metric ($dR@n, IoU@m$) can effectively reduce the inflating performance caused by the annotation biases when the IoU threshold m is small.

In summary, we make three contributions in this paper:

- We propose new splits of two prevailing TSGV datasets (Charades-CD and ActivityNet-CD), which are able to disentangle the effects of annotation biases.
- We propose a new evaluation metric $dR@n, IoU@m$, which is more reliable than the existing metrics, especially when the IoU threshold is small.
- We conduct extensive experiments with several SOTA models. Consistent performance gaps between IID and OOD samples have proven that the proposed splits and metric can better monitor the progress in TSGV.

2. Related Works

In this section, we review related works on TSGV from the following four categories.

Two-stage methods. Early TSGV works consider to solve this problem in a two-stage matching framework. They extract video segment candidates by temporal sliding windows, and then either match query sentence with these candidates [1] or fuse query and video segment features together to determine the final position via a regression network, e.g., CTRL [6], ACL-K [8], SLTA [12], ACRN [14], ROLE [15], and VAL [23]. To speed up the sliding window processing, Xu *et al.* proposed QSPN [30], which injects text features early to generate segment candidates. This can eliminate the unlikely segments and increase the grounding accuracy.

End-to-end methods. Besides the above two-stage framework, some other works seek to solve the grounding problem in an end-to-end manner [3, 31, 32, 33, 34, 35, 36]. Chen *et al.* proposed TGN [3], which sequentially scores a set of temporal candidates ended at each frame with LSTM networks and generates the final grounding result in one single pass. In addition, the ABLR model also processes video sequences via LSTMs [32], where the start and end points of the predicted segments are directly regressed from the attention weights yielded by the multi-pass interaction between videos and queries. There are also some works leveraging temporal convolutional networks to solve the TSGV problem. Zhang *et al.* presented MAN [34], which assigns candidate segment representations aligned with language semantics over different temporal locations and scales in hierarchical temporal convolutional feature maps. Yuan *et al.* introduced the SCDM [31], where query semantic is used to control the feature normalization between different temporal convolutional layers, making the query-related video activities tightly compose together. Both MAN and SCDM only consider 1D temporal feature maps, while the 2D-TAN network models the temporal relations between video segments by a two-dimensional map [35]. In the 2D map, 2D-TAN can encode the adjacent temporal relation, and further learn discriminative features for matching video segments with language queries.

Reinforcement learning based methods. Recently, reinforcement learning (RL) techniques [9, 10, 28, 29] have also been applied to the TSGV task. Specifically, Wang *et al.* introduced a semantic matching RL (SM-RL) model by extracting semantic concepts of videos and fusing them with global context features [28]. Then, video contents are selectively observed and associated with the given sentence in a matching-based manner. Hahn *et al.* presented TripNet, which uses RL to efficiently localize relevant activity clips in long videos, by learning how to intelligently skip around the video [9]. Wu *et al.* formulated a tree-structured policy based progressive RL (TSP-PRL) framework to sequentially regulate the temporal boundaries of predicted segments by an iterative refinement process [29].

Weakly supervised methods. Since the ground truth annotations for the TSGV task are consuming, some works start to extend this problem to a weakly supervised scenario where the ground truth segments are unavailable in the training stage [5, 7, 17, 24, 25]. Mithun *et al.* utilized a latent alignment between video frames and sentence descriptions with Text-Guided Attention (TGA), and TGA was then used during the test stage to retrieve relevant moments [17]. Duan *et al.* took the TSGV task as an intermediate step for dense video captioning, and then they established a cycle system and leveraged the captioning loss to train the whole model [5]. Song *et al.* presented a multi-level attentional reconstruction network [24], which leverages both intra-proposal (segment) and inter-proposal interaction to learn a language-driven attention map, which can directly score and rank the candidate proposals at the inference stage.

3. Dataset and Metric Analysis

3.1. Dataset Analysis

So far, there are four TSGV datasets having been proposed: DiDeMo [1], TACoS [20], Charades-STA [6] and ActivityNet Captions [13]. Since both DiDeMo and TACoS have some inherent and obvious disadvantages (*e.g.*, for DiDeMo dataset, the minimum interval of annotations is 5 seconds; for TACoS dataset, the visual scene is restricted in kitchen), the Charades-STA and ActivityNet Captions gradually become the mainstream benchmarks for evaluating the TSGV models [3, 9, 30, 31, 33, 35]. Therefore, we first perform a thorough analysis on these two datasets:

Charades-STA. It is built upon the Charades [22] dataset. The average length of videos in Charades is 30 seconds, and each video is annotated with multiple descriptions, action labels, action intervals, and classes of interacted objects. Gao *et al.* [6] extended the Charades dataset to the TSGV task by assigning the temporal intervals to text descriptions and matching the common key words in the interval action labels and texts. In the official split [6], there are 5,338

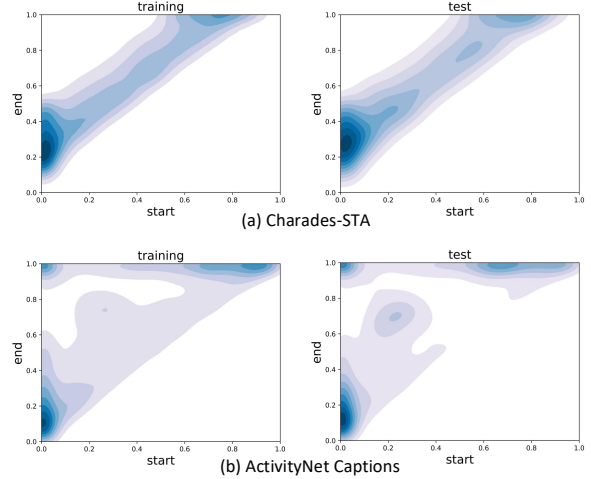


Figure 2. Moment annotation distributions of all query-moment pairs in both Charades-STA and ActivityNet Captions. The deeper the color, the larger density in the distribution.

videos and 12,408 query-moment pairs in the training set, and 1,334 videos and 3,720 query-moment pairs in the test set.

ActivityNet Captions. It is originally developed for dense video captioning [13]. Since the official test set is withheld for competitions, previous TSGV works [31, 32] merge the two available validation subsets “val1” and “val2” as the test set. In summary, there are 10,009 videos and 37,421 query-moment pairs in the training set, and 4,917 videos and 34,536 query-moment pairs in the test set.

To examine the moment annotation distributions of these two datasets, we normalize the start and end timestamps of all query-moment pairs in both the training and test sets, and use gaussian kernel density estimation to fit the joint distribution of the start and end points. As shown in Figure 2, for both two datasets, the moment annotation distributions are almost identical in their training and test sets. Specifically:

For Charades-STA, most of the moments start at the beginning of the videos and end at around 20% – 40% of the length of the videos. The moment annotation distributions present a strip with relatively uniform width, which indicates that the length of moment in Charades-STA roughly concentrates within a certain range. **For ActivityNet Captions,** the distributions are significantly different from those of Charades-STA, which is concentrated in three distinct areas, *i.e.*, the three corners. All these areas show that a considerable number of ground truth moments start at the beginning of the video or end at the ending of the video, even exactly the same as the whole video (the left top area). This is due to that the dataset ActivityNet Captions is originally annotated for dense video captioning, and the captions (queries) are always annotated based on the whole video.

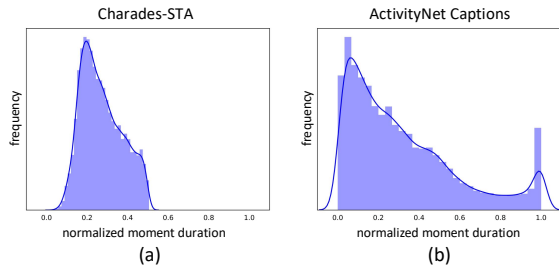


Figure 3. The histogram of the normalized moment duration in the Charades-STA and ActivityNet Captions datasets.

The distributions in other areas are more even, which means that the lengths of the moments are more diverse.

Therefore, all these characteristics provide strong prior knowledge about the ground truth moment annotations. By fitting these biases, a model even without training can still achieve a state-of-the-art performance (cf. Figure 1).

3.2. Metric Analysis

To evaluate the temporal grounding accuracy, previous TSGV works all adopt the “R@ n ,IoU@ m ” as a standard evaluation metric. Specifically, for each query q_i , it first calculates the Intersection-over-Union (IoU) between the location of predicted moment and its ground truth, and defines the metric R@ n ,IoU@ m as:

$$R@n, \text{IoU}@m = \frac{1}{N_q} \sum_i r(n, m, q_i), \quad (1)$$

where $r(n, m, q_i)$ equals to 1 if there is at least one of top- n predicted moments of query q_i having an IoU larger than threshold m , otherwise it equals to 0. N_q is the total number of all queries.

Most of previous TSGV methods [3, 15, 30, 32, 35] always report their scores on some small IoU thresholds like $m \in \{0.1, 0.3, 0.5\}$. However, as shown in Figure 3 (b), for dataset ActivityNet Captions, a substantial proportion of ground truth moments have very long durations. Statistically, 40%, 20%, and 10% of sentence queries refer to a moment occupying over 30%, 50%, and 70% of the length of the whole video, respectively. Such annotation biases can obviously increase the chance of correct prediction under small IoU thresholds. Taking an extreme case as example, if the ground truth moment is the whole video, any predictions with duration longer than 0.3 can achieve R@1, IoU@0.3 = 1. Thus, the metric R@ n ,IoU@ m with small m is unreliable for current biased annotated datasets.

4. Proposed Data Splits and Evaluation Metric

4.1. Dataset Re-splitting

To accurately monitor the research progress in TSGV and reduce the influence of biased annotations, we propose to re-organize these two datasets by deliberately assigning different moment annotation distributions in each split. Particularly, each dataset is re-splitted into four sets: training, validation (val), test-iid, and test-ood. All samples in the training, val, and test-iid satisfy the independent and identical distribution, and the samples in test-ood are out-of-distribution. The performance gap between the test-iid set and test-ood set can effectively reflect the generalization ability of the model. We name these two new re-organized datasets as **Charades-CD** and **ActivityNet-CD**.

Data aggregation and splitting. For each dataset, we combine all the query-moment pairs in each split, and use the gaussian kernel density estimation to fit the moment annotation distribution (cf. Figure 2). We rank all the samples based on their density values (from high to low) in the fitted distribution, and take the lowest 20% samples as the candidates of the test-ood set. By this design, we hope that the test-ood set contains samples with different annotation distributions from those in the training set.

Conflicting video elimination. Since each video is associated with multiple sentence queries, another concern is that we need to make sure that there is no video overlap between the training and test sets. Thus, after obtaining the candidate samples of the test-ood set, we check whether the videos of these samples also appear in the training set. If it is the case, we move all samples (*i.e.*, query-moment pairs) referring to the same video into the split with most of samples. In addition, to avoid the inflating performance of over-long predictions in ActivityNet (*e.g.*, the blind baseline which directly predicts the whole video as the moment), we put all samples with ground truth moment occupying over 50% of the length of the whole video into the training set.

After eliminating the conflicting videos, we obtain the test-ood set, which contains around 20% query-moment pairs of all samples. Then, we randomly divide the left samples into three sets: the training, val, and test-iid sets, which consist of around 70%, 5%, and 5% samples, respectively. The detailed statistics of the original and new proposed splits are reported in Table 1.

4.2. Charades-CD and ActivityNet-CD

Moment annotation distributions. The moment annotation distributions of Charades-CD and ActivityNet-CD are illustrated in Figure 4. From Figure 4, we can observe that the moment annotation distributions of the test-ood set are significantly different from those of the other three sets (*i.e.*, training, val, and test-iid). Compared with the moment annotation distributions of the original test split (cf. Figure 2),

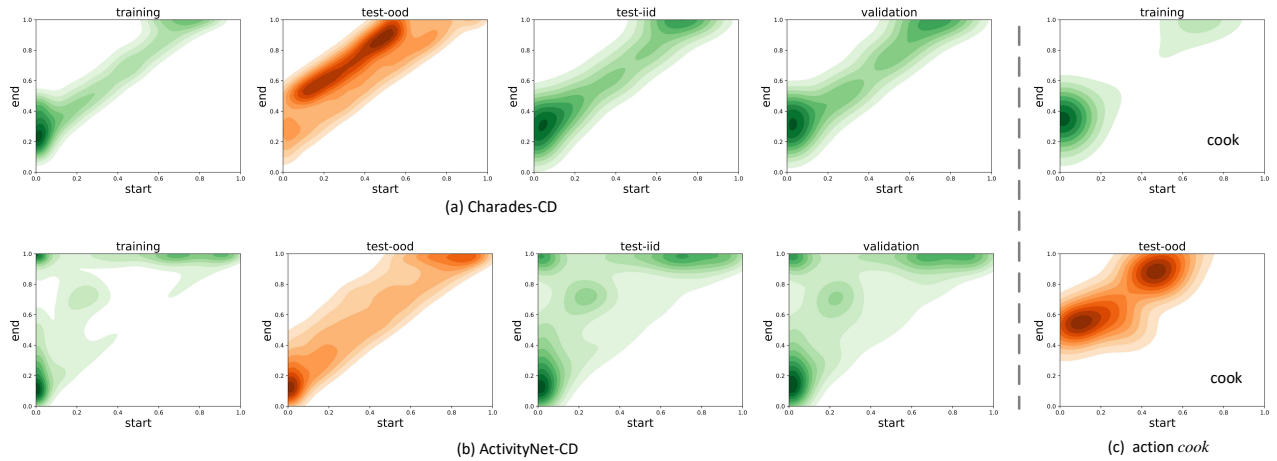


Figure 4. (a) and (b) illustrate the moment annotation distributions of each split in Charades-CD and ActivityNet-CD. (c) presents the moment annotation distributions of the query-indicated moments which contain action *cook* in the training and test-ood sets of Charades-CD. The deeper the color, the larger the density in the distribution.

| Dataset | Split | # Videos | # Pairs |
|----------------------|----------|----------|---------|
| Charades-STA | training | 5,338 | 12,408 |
| | test | 1,334 | 3,720 |
| ActivityNet Captions | training | 10,009 | 37,421 |
| | test | 4,917 | 34,536 |
| Charades-CD | training | 4,564 | 11,071 |
| | val | 333 | 859 |
| | test-iid | 333 | 823 |
| | test-ood | 1,442 | 3,375 |
| ActivityNet-CD | training | 10,984 | 51,415 |
| | val | 746 | 3,521 |
| | test-iid | 746 | 3,443 |
| | test-ood | 2,450 | 13,578 |

Table 1. The statistics of the number of videos and query-moment pairs in different datasets and splits.

the proposed test-ood split has several improvements: 1) for dataset Charades-CD, the distributions of the starting points of the moments are more diverse (vs. concentrating on the beginning of the videos; 2) for dataset ActivityNet-CD, more moments locate in relatively central areas of the videos, *i.e.*, the annotation biases are designed to be useless.

Action distributions. We further investigate the action distributions of the original and re-organized datasets. Specifically, for each dataset, we extract the verbs for all the sentence queries and count the frequency of each verb. Since the frequencies of all verbs obey a long-tail distribution, we select the top-30 frequent verbs, which cover 92.7% of all action types in Charades-CD and 52.9% for ActivityNet-CD, respectively. The statistical results are illustrated in Figure 5. From this figure, we can observe that the test-ood sets on both two datasets still have similar action distribu-

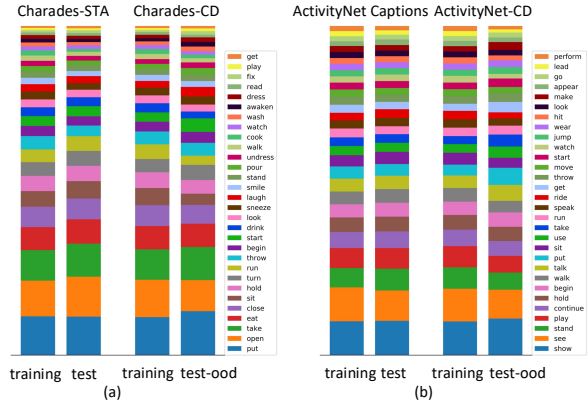


Figure 5. The frequency distributions of the top-30 actions in the query-moment pairs of each dataset split. The longer the bar, the more frequently the action appears.

tions to the training set and original splits, *i.e.*, the OOD of the moment annotations comes from each specific verb type. As the example shown in Figure 4(c), for all the sentence queries containing verb *cook*, the moment annotation distributions of the training set and test-ood set are totally different. We leave more visualization results of different verbs in the supplementary materials.

4.3. Proposed Evaluation Metric

As mentioned in Section 3.2, the prevailing evaluation metric R@ n ,IoU@ m is unreliable under small threshold m . To alleviate this problem, we propose to leverage the “temporal distance” between the predicted and ground truth moments to discount the $r(n, m, q_i)$ value, and propose a new

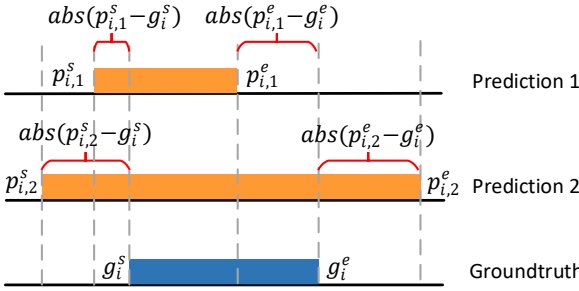


Figure 6. An illustration of the proposed dR@n,IoU@m metric. In this example, the IoU of the ground truth moment and two predictions (Prediction 1 and Prediction 2) are 0.5.

metric discounted-R@n,IoU@m (dR@n,IoU@m):

$$dR@n, \text{IoU}@m = \frac{1}{N_q} \sum_i r(n, m, q_i) \cdot \alpha_i^s \cdot \alpha_i^e, \quad (2)$$

where $\alpha_i^* = 1 - \text{abs}(p_i^* - g_i^*)$, and $\text{abs}(p_i^* - g_i^*)$ is the absolute distance between the boundaries of predicted and ground truth moments. Both p_i^* and g_i^* are normalized to 0-1 by dividing the whole video length. As shown in Figure 6, $(p_{i,1}^s, p_{i,1}^e)$ and $(p_{i,2}^s, p_{i,2}^e)$ denote two different predicted moments of query q_i , and (g_i^s, g_i^e) indicates the ground truth moment. When the predicted and ground truth moments are very close to each other, the discount ratio α_i^* will be close to 1, and the metric degrades to R@n,IoU@m. Otherwise, even the IoU threshold condition is met, the score $r(n, m, q_i)$ will still be discounted by α_i^* , which helps to restrain over-long predictions. As the example shown in Figure 6, both Prediction 1 and Prediction 2 meet the $\text{IoU} \geq 0.5$ condition, *i.e.*, these two predictions are regarded equally under the original R@n,IoU@m metric. However, since the temporal boundaries of the Prediction 2 is more far from the ground truth, the new metric will penalize more on the Prediction 2.

5. Experiments

5.1. Benchmarking the SOTA TSGV Methods

To demonstrate the difficulty of the new proposed splits (*i.e.*, Charades-CD and ActivityNet-CD), we compare the performance of two simple baselines and eight state-of-the-art methods on both the original and proposed splits. Specifically, we can categorize these methods into the following groups: 1) *Bias-based method*: it uses the gaussian kernel density estimation to fit the moment annotation distribution, and randomly samples several locations based on the fitted distribution as the moment predictions. 2) *PredictAll method*: it directly predicts the whole video as the moment predictions. 3) *Two-stage methods*: cross-modal temporal regression localizer (**CTRL**) [6], and attentive cross-

modal retrieval network (**ACRN**) [14]. 4) *End-to-end methods*: attention-based location regression (**ABLR**) [32], semantic conditioned dynamic modulation (**SCDM**) [31], 2D temporal adjacent network (**2D-TAN**) [35], and dense regression network (**DRN**) [33]. 5) *RL-based method*: tree-structured policy based progressive reinforcement learning (**TSP-PRL**) [29]. 6) *Weakly-supervised method*: weakly-supervised sentence localizer (**WSSL**) [5].

For all these SOTA methods, we use the public official implementations to get their temporal grounding results. The results of the proposed test-iid and test-ood sets on two datasets come from the same model finetuned on their respective val set. For more fair comparisons, we have unified the feature representations of the videos and sentence queries. To cater for most of TSGV methods, we use I3D feature [2] for the videos in Charades-STA (Charades-CD), and C3D feature [26] for the videos in ActivityNet Captions (Activity-CD). Each word in the query sentences is encoded by a GloVe [19] word representation.

5.2. Performance Comparisons on the Original and Proposed Data Splits

We report the performance of all mentioned TSGV methods with metric R@1,IoU@0.7 in Figure 7. From Figure 7, we can observe that almost all methods have a significant performance gap between the test-iid and test-ood sets, *i.e.*, these methods always over-rely on the moment annotation biases, and fail to generalize to the OOD test set. Meanwhile, the performance results on the original test set and the proposed test-iid set are relatively close, because the moment distribution of the test-iid set is still similar to the majority of the whole dataset. We provide more detailed experimental results analyses in the following:

Baseline methods. After changing the moment annotation distributions in different splits, the Bias-based method cannot take advantage of the annotation biases and its performance degrades from 13.6% on the test-iid set to 0.1% on the test-ood set of ActivityNet-CD. For the PredictAll method, since all the ground truth moments in Charades-CD are less than 50% range of the whole videos, just predicting the whole video as the grounding results will inevitably cause the R@1,IoU@0.7 scores to 0.0 on this dataset. Since the ground truth moments in ActivityNet-CD are much longer, the PredictAll method achieves high results at 11.9% and 13.8% on the original test set and new test-iid set, respectively. However, in the test-ood set where the longer segments are excluded, the PredictAll method also degrades its performance to 0.0.

Two-stage methods. We find that the two-stage methods (*i.e.*, both CTRL and ACRN) are less sensitive to the domain differences between the test-iid and test-ood sets. This is due to that they use a sliding window strategy to retrieve video moment candidates, and compare these moments with

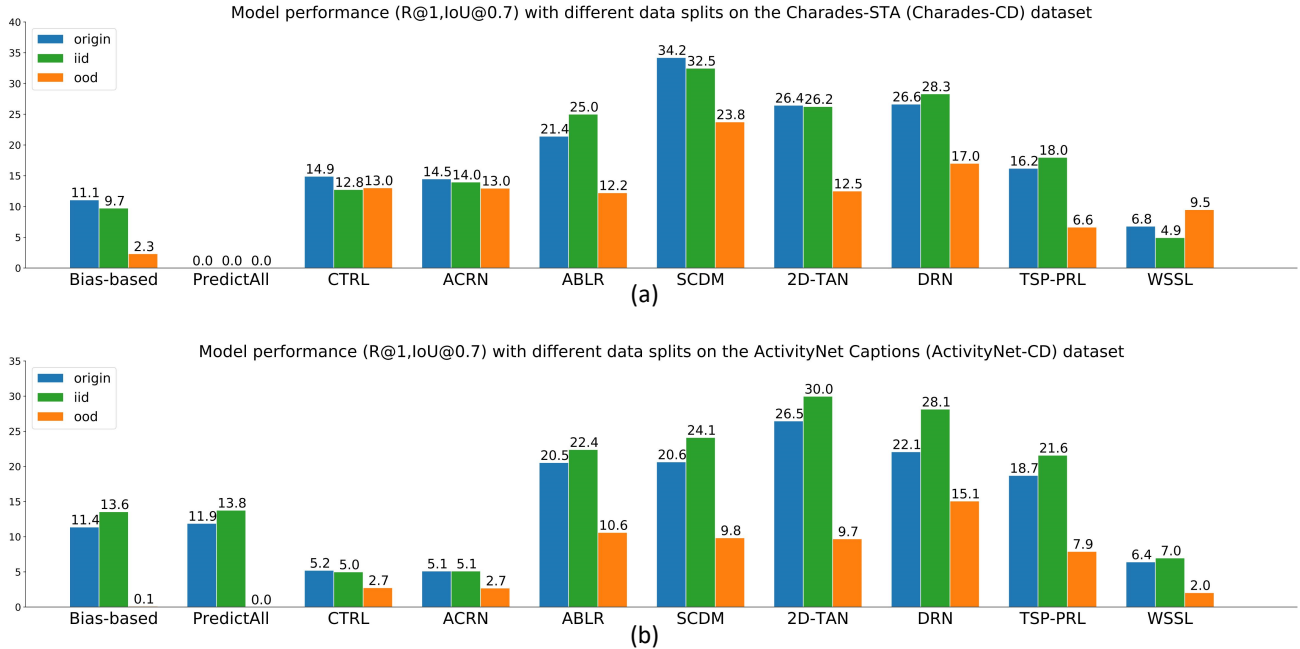


Figure 7. Performances (%) of SOTA TSGV methods on the test set of original splits (*i.e.*, Charades-STA and ActivityNet Captions) and test sets (test-iid and test-ood) of proposed splits (*i.e.*, Charades-CD and ActivityNet-CD). We use metric R@1,IoU@0.7 in all samples.

| Method | Split | Charades-CD | | | | | ActivityNet-CD | | | | |
|--------------|----------|-------------|-------|-------|-------|-------|----------------|-------|-------|-------|-------|
| | | m=0.1 | m=0.3 | m=0.5 | m=0.7 | m=0.9 | m=0.1 | m=0.3 | m=0.5 | m=0.7 | m=0.9 |
| Bias-based | test-iid | 31.42 | 26.25 | 16.87 | 9.34 | 2.70 | 36.15 | 29.31 | 19.81 | 12.27 | 7.68 |
| | test-ood | 14.75 | 9.30 | 5.04 | 2.21 | 0.55 | 21.89 | 9.21 | 0.26 | 0.11 | 0.03 |
| PredictAll | test-iid | 31.04 | 10.93 | 0.00 | 0.00 | 0.00 | 36.43 | 29.62 | 20.05 | 12.45 | 7.83 |
| | test-ood | 37.43 | 27.13 | 0.06 | 0.00 | 0.00 | 21.87 | 9.01 | 0.00 | 0.00 | 0.00 |
| CTRL [6] | test-iid | 50.61 | 42.65 | 29.80 | 11.86 | 1.41 | 27.34 | 19.42 | 11.27 | 4.29 | 0.25 |
| | test-ood | 52.80 | 44.97 | 30.73 | 11.97 | 1.12 | 26.23 | 15.68 | 7.89 | 2.53 | 0.20 |
| ACRN [14] | test-iid | 53.22 | 47.50 | 31.77 | 12.93 | 0.71 | 27.69 | 20.06 | 11.57 | 4.41 | 0.75 |
| | test-ood | 53.36 | 44.69 | 30.03 | 11.89 | 1.38 | 27.03 | 16.06 | 7.58 | 2.48 | 0.17 |
| ABLR [32] | test-iid | 59.26 | 52.26 | 41.13 | 23.50 | 3.66 | 55.62 | 46.86 | 35.45 | 20.57 | 6.32 |
| | test-ood | 54.09 | 44.62 | 31.57 | 11.38 | 1.39 | 46.88 | 33.45 | 20.88 | 10.03 | 2.31 |
| SCDM [31] | test-iid | 62.47 | 58.14 | 47.36 | 30.79 | 6.62 | 55.15 | 46.44 | 35.15 | 22.04 | 6.07 |
| | test-ood | 59.08 | 52.38 | 41.60 | 22.22 | 3.81 | 45.08 | 31.56 | 19.14 | 9.31 | 1.94 |
| 2D-TAN [35] | test-iid | 59.80 | 53.71 | 43.46 | 24.99 | 6.95 | 57.11 | 49.18 | 39.63 | 27.36 | 9.00 |
| | test-ood | 50.87 | 43.45 | 30.77 | 11.75 | 1.92 | 44.37 | 30.86 | 18.38 | 9.11 | 2.05 |
| DRN [33] | test-iid | 57.03 | 51.35 | 41.91 | 26.74 | 6.46 | 56.96 | 48.92 | 39.27 | 25.71 | 6.81 |
| | test-ood | 49.17 | 40.45 | 30.43 | 15.91 | 3.13 | 47.50 | 36.86 | 25.15 | 14.33 | 3.76 |
| TSP-PRL [29] | test-iid | 54.60 | 46.44 | 35.43 | 17.01 | 3.57 | 53.98 | 44.93 | 33.93 | 19.50 | 4.79 |
| | test-ood | 42.21 | 31.93 | 19.37 | 6.20 | 1.16 | 44.23 | 29.61 | 16.63 | 7.43 | 1.46 |
| WSSL [5] | test-iid | 45.90 | 34.99 | 14.06 | 4.27 | 0.00 | 36.67 | 26.06 | 17.20 | 6.16 | 1.24 |
| | test-ood | 49.92 | 35.86 | 23.67 | 8.27 | 0.06 | 30.71 | 17.00 | 7.17 | 1.82 | 0.17 |

Table 2. Performances (%) of SOTA TSGV methods on the Charades-CD and ActivityNet-CD datasets with metric dR@1,IoU@m.

each query sentence individually. In this manner, all moment candidates are independent to the overall video contents, and the moment annotation biases have less impact on the model performance. We can also observe that the performance of these two methods on the test-ood set of

ActivityNet-CD presents a more obvious drop compared to the test-iid set, while for Charades-CD, the performance on the test-iid and test-ood sets are competing. The reason is that the ground truth moments in the test-ood set of Charades-CD occupy a longer range in the whole videos

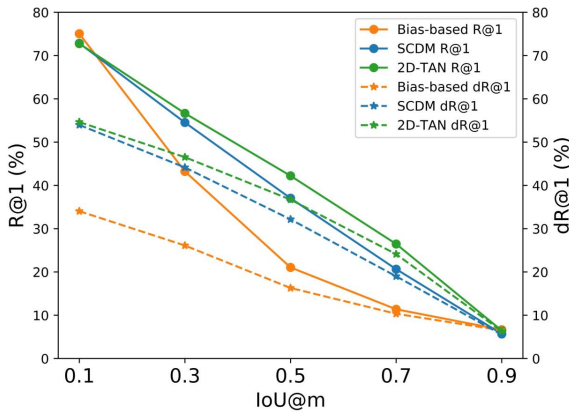


Figure 8. Performance comparisons between original metric ($R@1, \text{IoU}@m$) and proposed metric ($dR@1, \text{IoU}@m$). All results come from the test set of ActivityNet Captions.

(cf. Figure 4 (a)), which makes the sliding windows have more chance to hit the ground truth moments. In summary, although CTRL and ACRN are less sensitive to the moment annotation biases, their grounding performances are still far behind other SOTA methods, such as SCDM and DRN.

End-to-end methods. As for the end-to-end methods (*i.e.*, ABLR, SCDM, 2D-TAN and DRN), we can observe that their performances all drop significantly on the test-ood set compared to the test-iid set on both two datasets. These methods all have considered the whole video contexts and temporal information. The initial intention for this design is that some queries often contain some words referring to temporal orders and locations such as “before”, “after”, “begin” and “end”, or they think that the temporal relations between video moments are critical. However, such intention and the corresponding architectures do not play their advantages and hold the model performance on the out-of-distribution testing, even though the test-ood split does not break any video temporal relations and change the query-moment pairs. It is inevitable for these methods to learn the moment annotation biases from the training data. However, more attention should be paid to the true video temporal relation and vision-language interaction, instead of overly influenced by the temporal annotations.

RL-based method. The RL-based method TSP-PRL also suffers obvious performance drops on the test-ood set compared to the test-iid set. Actually, TSP-PRL adopts IoU between the predicted and ground truth moment as the training reward in the reinforcement learning framework. In this case, the temporal annotations directly affect the model learning, and changing the moment annotation distributions will inevitably cause the model performance degradation.

Weakly-supervised method. The results of the weakly-supervised method WSSL is thought-provoking: it achieves better performance on test-ood set compared to test-iid set

in Charades-CD, but results of these splits in ActivityNet-CD are exactly the reverse. After carefully checking the predicted moment results, we find that the normalized (start, end) moment predictions on both two datasets converge on several certain cases (*e.g.*, (0, 1), (0, 0.5), (0.5, 1)). These results indicate that the WSSL method is indeed not influenced by the moment annotation biases; however, it does not learn to align the video and sentence semantics, either, but speculatively guesses several possible locations.

5.3. Performance Evaluation with $dR@n, \text{IoU}@m$

We report the performance of all mentioned TSGV methods with our proposed metric ($dR@1, \text{IoU}@m$) in Table 2¹. The trend of performance drop on the test-ood set compared to the test-iid set is similar to that in Figure 7. Meanwhile, we can observe that the $dR@1, \text{IoU}@m$ values are smaller than the $R@1, \text{IoU}@m$ values. For example, the SCDM model achieves score 32.5% in $R@1, \text{IoU}@0.7$ while score 30.8% in $dR@1, \text{IoU}@0.7$ on the test-iid set of Charades-CD. For a clearer illustration, we further compare the $dR@1$ and $R@1$ scores under different IoUs of some methods in Figure 8. When the IoU threshold is small, $dR@1$ is much lower than $R@1$, and the gap between them gradually decreases when the IoU threshold increases. Interestingly, we find that Bias-based method achieves even better results than SCDM and 2D-TAN methods in the $R@1, \text{IoU}@0.1$ metric, while reversely in the $dR@1, \text{IoU}@0.1$ metric. The results indicate that recall values under small IoU thresholds are unreliable and overrated, because even if some predictions meet the IoU requirement, they still have a great discrepancy to the ground truth locations. Our proposed $dR@n, \text{IoU}@m$ metric can alleviate this problem since it can discount the recall value based on the temporal distance between the predicted and ground truth temporal locations. When the prediction meets the larger IoU requirements, the discount will be smaller, *i.e.*, the $dR@n, \text{IoU}@m$ and $R@n, \text{IoU}@m$ values will be closer to each other. Therefore, our predicted $dR@n, \text{IoU}@m$ metric is more stable on different IoU thresholds, and it can also suppress some inflating results (such as Bias-based method) caused by the moment annotation biases in the datasets. Meanwhile, these results further reveal that it is more reliable to report the grounding accuracy on large IoUs.

6. Conclusion

In this paper, we took a closer look at the existing evaluation protocol of the temporal sentence grounding in videos (TSGV) task, and we found that both the prevailing datasets and metrics are the devils to cause the unreliable benchmarking: the datasets have obvious moment annotation biases and the metric is prone to overrating the model perfor-

¹We leave more results in the supplementary material.

mance. To solve these problems, we proposed to re-split the current Charades-STA and ActivityNet Captions datasets by making the moment annotation distribution of the test set out of the distribution of the training set. Meanwhile, we proposed a new evaluation metric by discounting the performance on over-long predictions. The proposed data splits and metric serve as a promising test-bed to monitor the progress in TSGV. We evaluated eight state-of-the-art TSGV methods with the new evaluation protocol, opening the door for future research.

References

- [1] Lisa Anne Hendricks, Oliver Wang, Eli Shechtman, Josef Sivic, Trevor Darrell, and Bryan Russell. Localizing moments in video with natural language. In *ICCV*, 2017. [1](#), [2](#), [3](#)
- [2] Joao Carreira and Andrew Zisserman. Quo vadis, action recognition? a new model and the kinetics dataset. In *CVPR*, 2017. [6](#)
- [3] Jingyuan Chen, Xinpeng Chen, Lin Ma, Zequn Jie, and Tat-Seng Chua. Temporally grounding natural sentence in video. In *EMNLP*, 2018. [1](#), [2](#), [3](#), [4](#)
- [4] Long Chen, Chujie Lu, Siliang Tang, Jun Xiao, Dong Zhang, Chilie Tan, and Xiaolin Li. Rethinking the bottom-up framework for query-based video localization. In *AAAI*, 2020. [1](#)
- [5] Xuguang Duan, Wenbing Huang, Chuang Gan, Jingdong Wang, Wenwu Zhu, and Junzhou Huang. Weakly supervised dense event captioning in videos. In *NeurIPS*, 2018. [1](#), [3](#), [6](#), [7](#)
- [6] Jiyang Gao, Chen Sun, Zhenheng Yang, and Ram Nevatia. Tall: Temporal activity localization via language query. In *ICCV*, 2017. [1](#), [2](#), [3](#), [6](#), [7](#)
- [7] Mingfei Gao, Larry Davis, Richard Socher, and Caiming Xiong. Wslln: Weakly supervised natural language localization networks. In *EMNLP*, 2019. [1](#), [3](#)
- [8] Runzhou Ge, Jiyang Gao, Kan Chen, and Ram Nevatia. Mac: Mining activity concepts for language-based temporal localization. In *WACV*, 2019. [1](#), [2](#)
- [9] Meera Hahn, Asim Kadav, James M Rehg, and Hans Peter Graf. Tripping through time: Efficient localization of activities in videos. In *arXiv*, 2019. [1](#), [3](#)
- [10] Dongliang He, Xiang Zhao, Jizhou Huang, Fu Li, Xiao Liu, and Shilei Wen. Read, watch, and move: Reinforcement learning for temporally grounding natural language descriptions in videos. In *AAAI*, 2019. [1](#), [3](#)
- [11] Lisa Anne Hendricks, Oliver Wang, Eli Shechtman, Josef Sivic, Trevor Darrell, and Bryan Russell. Localizing moments in video with temporal language. In *EMNLP*, 2018. [1](#)
- [12] Bin Jiang, Xin Huang, Chao Yang, and Junsong Yuan. Cross-modal video moment retrieval with spatial and language-temporal attention. In *ICMR*, 2019. [1](#), [2](#)
- [13] Ranjay Krishna, Kenji Hata, Frederic Ren, Li Fei-Fei, and Juan Carlos Niebles. Dense-captioning events in videos. In *ICCV*, 2017. [1](#), [2](#), [3](#)
- [14] Meng Liu, Xiang Wang, Liqiang Nie, Xiangnan He, Baoquan Chen, and Tat-Seng Chua. Attentive moment retrieval in videos. In *SIGIR*, 2018. [1](#), [2](#), [6](#), [7](#)
- [15] Meng Liu, Xiang Wang, Liqiang Nie, Qi Tian, Baoquan Chen, and Tat-Seng Chua. Cross-modal moment localization in videos. In *ACM MM*, 2018. [1](#), [2](#), [4](#)
- [16] Chujie Lu, Long Chen, Chilie Tan, Xiaolin Li, and Jun Xiao. Debug: A dense bottom-up grounding approach for natural language video localization. In *EMNLP*, 2019. [1](#)
- [17] Niluthpol Chowdhury Mithun, Sujoy Paul, and Amit K Roy-Chowdhury. Weakly supervised video moment retrieval from text queries. In *CVPR*, 2019. [3](#)
- [18] Mayu Otani, Yuta Nakashima, Esa Rahtu, and Janne Heikkilä. Uncovering hidden challenges in query-based video moment retrieval. In *BMVC*, 2020. [1](#)
- [19] Jeffrey Pennington, Richard Socher, and Christopher D Manning. Glove: Global vectors for word representation. In *EMNLP*, 2014. [6](#)
- [20] Michaela Regneri, Marcus Rohrbach, Dominikus Wetzel, Stefan Thater, Bernt Schiele, and Manfred Pinkal. Grounding action descriptions in videos. In *TACL*, 2013. [1](#), [3](#)
- [21] Zheng Shou, Dongang Wang, and Shih-Fu Chang. Temporal action localization in untrimmed videos via multi-stage cnns. In *CVPR*, 2016. [1](#)
- [22] Gunnar A Sigurdsson, GÜl Varol, Xiaolong Wang, Ali Farhadi, Ivan Laptev, and Abhinav Gupta. Hollywood in homes: Crowdsourcing data collection for activity understanding. In *ECCV*, 2016. [3](#)
- [23] Xiaomeng Song and Yahong Han. Val: Visual-attention action localizer. In *PCM*, 2018. [2](#)
- [24] Yijun Song, Jingwen Wang, Lin Ma, Zhou Yu, and Jun Yu. Weakly-supervised multi-level attentional reconstruction network for grounding textual queries in videos. In *arXiv*, 2020. [3](#)
- [25] Reuben Tan, Huijuan Xu, Kate Saenko, and Bryan A Plummer. wman: Weakly-supervised moment alignment network for text-based video segment retrieval. In *arXiv*, 2019. [3](#)

- [26] Du Tran, Lubomir Bourdev, Rob Fergus, Lorenzo Torresani, and Manohar Paluri. Learning spatiotemporal features with 3d convolutional networks. In *ICCV*, 2015. [6](#)
- [27] Limin Wang, Yuanjun Xiong, Zhe Wang, Yu Qiao, Dahua Lin, Xiaoou Tang, and Luc Van Gool. Temporal segment networks: Towards good practices for deep action recognition. In *ECCV*, 2016. [1](#)
- [28] Weineng Wang, Yan Huang, and Liang Wang. Language-driven temporal activity localization: A semantic matching reinforcement learning model. In *CVPR*, 2019. [1, 3](#)
- [29] Jie Wu, Guanbin Li, Si Liu, and Liang Lin. Tree-structured policy based progressive reinforcement learning for temporally language grounding in video. In *AAAI*, 2020. [1, 3, 6, 7](#)
- [30] Huijuan Xu, Kun He, Bryan A Plummer, Leonid Sigal, Stan Sclaroff, and Kate Saenko. Multilevel language and vision integration for text-to-clip retrieval. In *AAAI*, 2019. [1, 2, 3, 4](#)
- [31] Yitian Yuan, Lin Ma, Jingwen Wang, Wei Liu, and Wenwu Zhu. Semantic conditioned dynamic modulation for temporal sentence grounding in videos. In *NeurIPS*, 2019. [1, 2, 3, 6, 7](#)
- [32] Yitian Yuan, Tao Mei, and Wenwu Zhu. To find where you talk: Temporal sentence localization in video with attention based location regression. In *AAAI*, 2019. [1, 2, 3, 4, 6, 7](#)
- [33] Runhao Zeng, Haoming Xu, Wenbing Huang, Peihao Chen, Mingkui Tan, and Chuang Gan. Dense regression network for video grounding. In *CVPR*, 2020. [1, 2, 3, 6, 7](#)
- [34] Da Zhang, Xiyang Dai, Xin Wang, Yuan-Fang Wang, and Larry S Davis. Man: Moment alignment network for natural language moment retrieval via iterative graph adjustment. In *CVPR*, 2019. [1, 2](#)
- [35] Songyang Zhang, Houwen Peng, Jianlong Fu, and Jiebo Luo. Learning 2d temporal adjacent networks for moment localization with natural language. In *AAAI*, 2020. [1, 2, 3, 4, 6, 7](#)
- [36] Zhu Zhang, Zhijie Lin, Zhou Zhao, and Zhenxin Xiao. Cross-modal interaction networks for query-based moment retrieval in videos. In *SIGIR*, 2019. [1, 2](#)